Environmentally Induced Sperm RNAs Transmit Cancer Susceptibility to Offspring in a Mouse Model

Raquel Santana da Cruz[1], Odalys Dominguez[1] , Elaine Chen[1], Alexandra K. Gonsiewski [1], Apsra Nasir[1], M. Idalia Cruz[1], Xiaojun Zou[1], Susana Galli[1], Kepher Makambi[1,2], Matthew McCoy[1], Marcel O. Schmidt[1], Lu Jin[1], Ivana Peran[1], and Sonia de Assis[1]*

[1]Department of Oncology, Lombardi Comprehensive Cancer Center, Georgetown University, Washington, DC, USA.

[2]Department of Biostatistics, Bioinformatics, & Biomathematics, Georgetown University, Washington, DC, USA.

***Corresponding author:** Sonia de Assis, Ph.D., 3970 Reservoir Road, NW, The Research Building, Room E410, Washington, DC 20057, USA; Phone: (202) 687-9518, Fax: (202) 687-7505, Email: deassiss@georgetown.edu, ORCID: 0000-0001-5053-0614

The authors declare they have no actual or potential competing financial interests

Abstract

DNA sequence accounts for the majority of disease heritability, including cancer. Yet, not all familial cancer cases can be explained by genetic factors. It is becoming clear that environmentally induced epigenetic inheritance occurs and that the progeny's traits can be shaped by parental environmental experiences. In humans, epidemiological studies have implicated environmental toxicants, such as the pesticide DDT, in intergenerational cancer development, including breast and childhood tumors. Here, we show that the female progeny of males exposed to DDT in the pre-conception period have higher susceptibility to developing aggressive tumors in mouse models of breast cancer. Sperm of DDT-exposed males exhibited distinct patterns of small non-coding RNAs, with an increase in miRNAs and a specific surge in miRNA-10b levels. Remarkably, embryonic injection of the entire sperm RNA load of DDT-exposed males, or synthetic miRNA-10b, recapitulated the tumor phenotypes observed in DDT offspring. Mechanistically, miR-10b injection altered the transcriptional profile in early embryos with enrichment of genes associated with cell differentiation, tissue and immune system development. In adult DDT-derived progeny, transcriptional and protein analysis of mammary tumors revealed alterations in stromal and in immune system compartments. Our findings reveal a causal role for sperm RNAs in environmentally induced inheritance of cancer predisposition and, if confirmed in humans, this could help partially explain some of the "missing heritability" of breast, and other, malignancies.

Introduction

Family history is one of the most important risk factors for cancer. A number of germline mutations are causally linked to familial cancer syndromes. Yet, not all familial cancer cases can be explained by high penetrance genes mutations. Genome-wide association studies (GWAS) of variants have been able to account for a fraction of familial cancer predisposition, but much of the "missing" cancer heritability remains unexplained.(1)

Accumulating evidence suggests that parental life experiences can affect the progeny's predisposition to disease in an epigenetically inherited manner. (2,3) At conception, parents not only contribute their genome but also transmit a molecular memory of past environmental experiences to the offspring. (2,4) This environmentally-induced disease predisposition has been shown to be transmitted to the offspring via epigenetic mechanisms through both the female and male germ-lines. (5-7) Although most of the evidence for this mode of disease inheritance comes from maternal exposures in pregnancy, a number of independent studies have shown that paternal exposures in the pre-conception window are also important in determining disease outcomes in the offspring. (8-14)

Several recent published reports demonstrated that the sperm RNA load can transmit environmentally-induced phenotypes from fathers to offspring. (2,7,15,16) Some of these studies implicate specific classes of sperm small non-coding RNAs, such as miRNAs and tRNA fragments (tRFs), which can recapitulate the effect of specific paternal exposures in offspring when injected into normal embryos following fertilization. (15-19)

Population studies link parental exposures to environmental pesticides with both childhood and adult cancers in the progeny (20-29). For instance, the epidemiologic analysis using the Child Health and Development Studies cohort (CHDS) found that daughters of women exposed to high

levels of dichlorodiphenyltrichloroethane (DDT) in pregnancy are more likely to have increased rates of breast cancer (20,30) and to be diagnosed with advanced stage tumors. (20)

Though the use of DDT has been restricted in many countries for decades, developing countries with endemic malaria, and other vector-borne diseases, continue to use it. (20,31-33) In countries where it has been banned, this pesticide is a persistent organic environmental pollutant and an endocrine disruptor. (31,34) Because of its low degradation rates and lipophilic properties, DDT bio-accumulates in the food chain, and can still be detected in fatty tissues and circulation of animals and humans in these countries. (31) In the U.S., the highest concentrations of DDT metabolites are found in minority populations and recent immigrants.(35,36)

Despite strong association between parental exposures to environmental toxins and cancer in the next generation, the precise mechanisms underlying this association remain unknown. Here, using mouse models of breast cancer, we tested the hypothesis that paternal exposure to DDT alters the sperm non-coding RNA load and increases cancer susceptibility in the next generation. We also examined whether paternal DDT-induced programming of breast cancer development in daughters is mechanistically linked to sperm non-coding RNAs and the underlying mechanisms.

Results

Paternal exposure to the environmental toxicant DDT leads to enhanced breast tumor growth in offspring

Parental exposure to environmental toxicants such as DDT and other pesticides has been associated to cancer development, including breast tumors, in the next generation. (20,22,28) To test whether we could replicate these findings in an animal model, adult male mice were either exposed to a vehicle-control (CO) or an environmentally relevant dose of DDT and, subsequently,

mated with unexposed females to generate the progeny (**Fig. 1a**). Using the well-established DMBA-induced mouse model of breast cancer, (8,37) we examined mammary cancer development in the female progeny of CO and DDT exposed fathers. Tumor growth was significantly increased in female offspring of DDT exposed fathers (referred to as 'DDT offspring' from this point on) compared to CO (**Fig. 1b**), with significantly higher tumor burden and tumor weight at the end of the monitoring period (**Fig. 1c, Fig. S1**). Although not significantly different, the incidence and latency of mammary tumors was slightly higher and shorter, respectively, in DDT offspring compared to CO (**Fig. 1d-e**).

To test whether the increase in carcinogen-induced mammary tumor growth observed in DDT offspring could be replicated in a different *in vivo* system, we used a syngeneic orthotopic mouse model of breast cancer. Consistent with our observations in the carcinogen-induced model, we found that EO771 murine breast cancer cells implanted in mammary fat pads of DDT offspring also resulted in significantly higher tumor growth compared to CO (**Fig. 1f-g**).

Sperm RNAs contribute to DDT-induced paternal transmission of breast cancer predisposition to offspring

The sperm RNA load, which is abundant in small non-coding RNAs,(38) was previously thought to be a non-functional remnant of the spermatogenesis process. However, several reports show that sperm RNAs can alter early embryonic development, and they have been recently linked to transmission of phenotypes in a variety of disease models. (17-19,39)

To assess whether sperm RNAs are associated with the increased cancer development in DDT offspring, the RNA load extracted from mature sperm of either DDT-exposed or CO male mice was injected into normal mouse embryos at the zygote stage. Injected embryos were then

transferred into surrogate dams to generate the DDT-sperm RNA and CO-sperm RNA offspring (**Fig.2a**). Remarkably, DMBA-induced mammary tumors grew significantly larger in DDT-sperm RNA female offspring than in the CO-sperm RNA group (**Fig. 2b-c**), recapitulating the original phenotype observed in DDT offspring. Consistent with results in DDT offspring, we also observed a non-significant increase in tumor incidence and shorter tumor latency in DDT-sperm RNA offspring (**Fig. 2d-e**).

Our findings were further confirmed in an orthotopic mouse model of breast cancer. Mammary fat pad injection of EO771 cells resulted in increased mammary tumor growth in DDT-sperm RNA female offspring, which had significantly increased tumor volume over time with increased tumor percentage growth at the end of the monitoring period compared to CO-sperm RNA offspring (**Fig 2f-g**).

Pre-conception paternal exposure to DDT alters the sperm non-coding RNA content

While mature sperm is transcriptionally inactive, recent studies show that, following testicular exit, the mammalian sperm acquires a load of small non-coding RNAs during transit in the epididymis,(40) the last stage of sperm maturation. Importantly, this non-coding RNA load is sensitive to environmental insults.(2,10,19) To determine the impact of DDT exposure on the mouse sperm RNA content, we performed RNA-seq analysis to profile small RNAs in sperm collected from CO and DDT-exposed mice (**Fig. 3a**). The distribution of the major small RNA species detected in the sperm is in line with previous reports, (18,39) with tRNA-derived fragments (tRFs) being the most abundant small RNA sub-type, followed by miRNAs and other RNAs in both groups (**Fig. 3b**).

141 We found that sperm of DDT-exposed males showed higher abundance of miRNAs reads
142 (7%) compared to the CO group (3%) (**Fig. 3b**). A total of 23 miRNAs were differentially
143 expressed (six down- and seventeen upregulated) in sperm of DDT-exposed mice compared to CO
144 (**Fig. 3c**). Among the upregulated miRNAs, miRNA-10b had the highest surge, representing close
145 to three quarters of the differentially expressed miRNA normalized counts in sperm of DDT-
146 exposed males compared to about half of the reads in the CO group (**Fig. 3d-e**). This is consistent
147 with a recent report showing that miRNA-10b is one the main miRNAs acquired by sperm cells
148 during epididymal transit. (40)

149 To establish whether regulation of miRNAs in sperm was, in fact, induced by DDT
150 exposure, we treated DDT-exposed mice with phenobarbital (PB, **Fig.4a**), a drug known to
151 promote hepatic enzymes activation and accelerate DDT metabolism and excretion in humans
152 (41,42) and animals. (43-45) Indeed, we observed a sharp increase in the hepatic phase I enzyme,
153 Cyp2B10, mRNA levels (**Fig.4b**) and a reduction in DDT main metabolites in DDT-exposed males
154 also treated with PB (**Fig.4c**).

155 Next, we investigated the effects of PB treatment on miRNAs that were differentially
156 expressed in sperm of DDT-exposed mice. For greater reliability, our analysis focused on the nine
157 differentially expressed miRNAs, which had an average of at least 100 normalized read counts
158 in our original RNA-seq data.

159 Compared to mice in the DDT-exposed group, miRNA-10b levels were significantly
160 reversed in sperm of mice treated with both DDT and PB (DDT+PB) with levels returning to those
161 observed in controls (CO and CO+PB) both by RNA-seq and q-PCR (**Fig. 4d-e**).

162 In addition to miRNA-10b, levels of miRNA-182-5p, miRNA-205-5p, and miRNA-375-
163 3p were also reversed by PB treatment in sperm of DDT-exposed males in the RNA-seq analysis,

though these findings could not be confirmed by q-PCR (**Fig. S3**). The expression levels of the five remaining miRNAs— including miR-6240, which had the sharpest decrease—were not reversed by PB treatment (**Fig. 4d** and **Fig. S3**), suggesting that they may not be DDT-specific.

Because tRFs have also been linked to intergenerational transmission of phenotypes, (15,16) we also investigated these small RNAs in sperm of DDT-exposed males via RNA-seq analysis. We found nine tRFs differentially expressed (one upregulated and eight downregulated) in sperm of DDT-exposed mice. However, these differentially expressed tRFs are likely not DDT-specific as they were not reversed by PB treatment and could not be confirmed in the follow-up analysis (**Fig. S4**).

miRNA-10b embryonic injection recapitulates tumor phenotypes observed in offspring of DDT-exposed fathers

To further validate the functional importance of miRNA-10b to phenotypes observed in DDT offspring, we injected synthetic miR-10b or controls (scramble-miR or vehicle solution) into normal mouse zygotes. Injected embryos were then transferred into surrogate dams to generate the miR-10b and CO offspring (**Fig. 5a**). The resulting miR-10b female offspring showed increased orthotopic (EO771 cells) mammary tumor development, with higher tumor growth compared to both control groups (vehicle injection or scrambled miR, **Fig. 5b**). The miR-10b females also had higher tumor burden and weight compared to the scrambled group (**Fig. 5c, Fig. S5**), at the end of the monitoring period.

Because small RNAs driven alterations in early embryonic development can have long lasting consequences and affect adult phenotype(19), we next examined whether embryonic injection of miR-10b at the zygote stage reshaped the mouse transcriptome profile at the blastocyst

stage (E3.5), using bulk RNA-sequencing (**Fig. 5d, Table S1**). We first assessed whether differentially expressed genes (DEG) were potentially regulated by miR-10b. In total, 63 genes down-regulated in miR-10b injected embryos are predicted targets of miR-10b (**Table S2**). Next, we performed a functional annotation analysis to identify the biological signatures most strongly associated with DEGs in miR-10b injected embryos compared to CO. We found an enrichment for terms related to embryonic, cell, tissue and organ development and cell differentiation as well as abnormal hematopoietic and immune system development in miRNA-10b injected embryos (**Fig. 5e)**. Among DEGs involved in immune response several are predicted targets of miR-10b, including *Ifng*, *Mmp25*, I*gsf23*, *Lrrc8b*, *Mtcp1*and *Nfam*.

Tumors of DDT-derived offspring have distinct signaling programs and alterations in the stromal and immune compartments.

To define the molecular changes underlying the increased cancer growth phenotype in DDT, DDT-sperm RNA and miR-10b offspring (collectively referred to as DDT-derived offspring from this point on), we performed a bulk RNA-sequencing analysis, followed by a gene set enrichment analysis (GSEA) of DEG, in their tumors. The GSEA revealed several significantly downregulated pathways in DDT-derived offspring tumors compared to CO, including epithelial mesenchymal transition (EMT), interferon gamma (IFN-γ) response and allograft rejection pathways (**Fig. 6a, Fig. S6, Tables S3A-3C**).

Our imaging mass cytometry (IMC) analysis confirmed alterations in EMT-associated proteins with a decrease in the extracellular matrix protein collagen type I expression (**Fig. 6b, Fig. S6**) and an increase in α-Smooth Muscle Actin (α-SMA; **Fig. 6c, Fig. S6**) in carcinogen-induced tumors of DDT-derived offspring. Orthotopic tumors generally have a less organized

stromal architecture, and although we observed a reduction in collagen type I in EO771 tumors of DDT-derived offspring, the results were not statistically significant.

To confirm the downregulation of immune-related pathways in tumors of DDT-derived offspring, we next investigated whether there were differences in the tumor immune cell infiltrates between the groups, but no consistent differences were detected. Because the IFN-γ signaling has been shown to be a dominant driver of PD-L1 expression in many tumor types,(46) we then examined the levels of this protein in tumors of DDT-derived offspring compared to CO. In line with the downregulation of the IFN-γ response pathway in the transcriptome analysis, we found a significant decrease in PD-L1 protein expression levels in carcinogen-induced tumors—and a trend towards decrease in orthotopic tumors—of DDT-derived offspring compared to CO (**Fig. 6d**).

Discussion

Family history is one of the most important risk factors for cancer. Yet, not all familial cancer cases can be explained by germline genetic mutations.(1) While there is agreement that the interplay between the environment and genetic factors could also contribute to cancer predisposition, much of the "missing" cancer heritability remains unexplained.

Growing evidence suggests that environmentally induced epigenetic inheritance occurs in mammals and that the progeny's traits can be shaped by parental environmental experiences.(17,18,39) The findings presented here lend support to this concept: Our study showed that pre-conception paternal exposure to an environmentally relevant dose of the pesticide DDT modulates the sperm non-coding RNA load, particularly miRNAs, and programs female offspring's breast cancer development and growth in a carcinogen-induced mouse model. These

233 results were substantiated in an orthotopic mouse model of breast cancer. We also showed that
234 sperm RNAs are functionally linked to the cancer phenotypes observed in offspring and
235 demonstrated that embryo injection of total sperm RNA from DDT-exposed males or synthetic
236 miRNA-10b, the miRNA with the highest increase in sperm of DDT-exposed fathers, recapitulated
237 the mammary tumor phenotypes observed in DDT daughters.

238 Our findings —that adult DDT exposure alters the non-coding small RNA load in sperm—
239 are consistent with other reports showing that environmental insults can modify sperm RNA
240 cargo.(7,17,19) While the proposed mechanisms are still being investigated, recent reports suggest
241 that sperm cells acquire their small RNA load as they transit through the reproductive system and
242 that extra cellular vesicles produced by epididymal cells play a role in this process.(39,47)
243 Furthermore, it has been proposed that during the normal fertilization process, sperm small RNAs
244 are delivered to the oocyte and modulate the transcriptome during the first few cell divisions,
245 setting a signaling cascade that can continue to impact embryonic development. (48) This ripple
246 effect disturbs regulatory networks in the developing embryo which can result in permanent
247 alterations in specific organs.(2,19) In line with this, embryonic injection of sperm RNAs from
248 DDT-exposed male or synthetic miRNA-10b replicates the major tumor phenotypes observed in
249 DDT daughters and transcriptional changes can be detected in pre-implantation embryos injected
250 with miR-10b.

251 Though we focused on the male germline in our study, it is important to note that
252 environmentally-induced epigenetic alterations likely also occur in the female germline. However,
253 it is technically challenging to directly examine maternal germline effects due to the scarcity of
254 eggs in both rodent and human females as well as the potential confounding of pregnancy
255 exposures.

256 In our mouse model, DDT offspring appear normal under basal conditions but become
257 more vulnerable to cancer development upon being challenged with a carcinogen or implanted
258 with tumorigenic cells. This suggests that ancestrally acquired traits manifest upon further post-
259 natal insults, acting in synergy to increase cancer susceptibility in offspring. It is possible that the
260 mammary tumor phenotype in DDT-derived offspring results from alterations in immune response
261 (down regulation of genes involved in IFN-γ signaling and reduced PD-L1 levels) and in the
262 mammary stroma (reduced collagen type I). It has been reported that loss of collagen type I is
263 functionally linked to rapid tumor growth and immune suppression. (49) Furthermore, PD-L1
264 levels has been show to correlate with EMT markers in different solid tumors types.(46)
265 Nonetheless, how, and at what stage of development, these underlying molecular events take place
266 in DDT-derived offspring needs to be further examined. Our data indicates that these alterations
267 may begin in early embryonic development as downregulation of *Ifng* and other immune
268 associated genes are detected in miRNA-10b injected embryos. However, it remains to be
269 determined whether reduction in IFN-γ signaling is maintained throughout development and
270 whether functionally impacts outcomes in vivo.

271 Our study revealed that miRNAs constituted the main small RNA subtype altered by DDT
272 exposure, with a specific DDT-induced surge in sperm miRNA-10b. This miRNA, along with
273 other members of the miRNA-10 family, plays a critical role in embryonic development and cell
274 differentiation through the regulation of Homeobox (*Hox*) and other genes. (50) Interestingly,
275 studies examining different paternal environmental exposures including obesity and malnutrition
276 report an upregulation of miRNA-10b and other members of the miR-10 family in sperm.
277 (9,10,18,51) It has also been reported that both sperm miRNA-10a and miRNA-10b are conserved
278 across species including humans.(52) These miRNAs are acquired by sperm cells during

279 epididymal transit in mice,(40) suggesting that alterations in their expression could potentially act
280 as a "sensor" of paternal environments.

281 While life-style factors such as obesity have been shown to alter sperm non-coding RNAs
282 in men,(53) no human studies have directly investigated the link between environmental toxicants
283 such as DDT and germline RNA changes to the best of our knowledge; though several reports in
284 animal models exist.(54-56) Nonetheless, a number of epidemiological studies link parental
285 environmental toxins and cancer in the progeny. For instance, an association between paternal
286 exposure to pesticides and a number of childhood cancers in offspring has been reported. (22-29)
287 Furthermore, published reports using the CHDS cohort showed that maternal exposure to DDT
288 increases rates of breast cancer in daughters who are also more likely to be diagnosed with
289 advanced-stage tumors. (20) Another recent population study using a historical cohort showed that
290 paternal grandfathers' nutrition leads to a transgenerational increase in cancer mortality rates in
291 grandsons.(57)

292 In summary, our study shows that the environmentally induced alterations in paternal
293 sperm non-coding RNAs are functionally linked to increased cancer susceptibility in the progeny.
294 Though our results are intriguing and suggest that cancer predisposition could be determined via
295 epigenetic inheritance, many questions still remain: For instance, how sperm non-coding RNAs
296 and miR-10b specifically alter early embryonic development to disrupt offspring's systemic and
297 mammary specific development needs to be further examined. Although epidemiologic studies
298 strongly suggest it, whether this phenomenon is restricted to breast tumors or whether it applies to
299 other malignancies needs confirmation in additional experimental models.

300 According to published studies and the Center for Disease Control and Prevention (CDC),
301 minorities such as African Americans and Mexican-Americans and recent immigrants have the

highest circulating concentrations of DDT metabolites and other environmental toxins in the U.S. (35,36,58) . Thus, our findings are likely relevant to other environmental pollutants which, like DDT, have endocrine disrupting properties(59-61) and could have important implications for cancer disparities.

Materials and Methods

DDT exposures and breeding: The *c57bl/6* strain of mice was used in all experiments. Adult male mice (8 weeks of age) were either treated daily with a DDT solution (1.7 mg/kg) or vehicle-control solution (peanut oil) via oral gavage for 17 days. Duration of exposures was chosen in order to encompass the entire period of sperm transit in the epididymis (which takes about 15 days in mammals) and when the sperm acquire its mature non-coding RNA load (62). The DDT solution used mimics the formulation of DDT before its ban in the U.S.: 77.2% p,p'-DDT and 22.8% o,p'-DDT as described before (63). Mice body weight was monitored weekly. At the end of the exposure period, DDT-exposed and control male mice were mated to unexposed females to generate the female offspring. Mice were kept on a standard chow diet during the breeding period, for the extent of pregnancy (21 days) and after birth. To avoid litter-effect, pups were cross-fostered one day after birth. Pups from 2-3 dams were pooled and housed in a litter of 8-10 pups per nursing dam. All pups were weaned on postnatal day (PND) 21. The female offspring of control or DDT-exposed fathers were used to study mammary tumorigenesis and for tissue collection as described in the following sections. All animal procedures were approved by the Georgetown University Animal Care and Use Committee, and the experiments were performed following the National Institutes of Health guidelines for the proper and humane use of animals in biomedical research. All exposures were performed blindly.

325 ***DDT and Phenobarbital (PB) treatment:*** PB treatment is known to promote hepatic enzymes
326 activation, accelerating DDT metabolism and excretion in humans (41,42) and animals (43-45). A
327 sub-set of control-vehicle (CO) or DDT exposed male mice (as above) were concomitantly treated
328 with phenobarbital (20 mg/kg of body weight, i.p.) or saline and used for sperm harvesting.

329 ***Mature spermatozoa collection and purification:*** CO and DDT-exposed male mice as well as
330 those concomitantly treated with PB were euthanized and caudal epididymis dissected for sperm
331 collection. The epididymis was collected, punctured, and transferred to a tissue culture dish
332 containing M2 media (M2 Medium-with HEPES, without penicillin and streptomycin, liquid,
333 sterile-filtered, suitable for mouse embryo, SIGMA, product #M7167) where it was incubated for
334 1 hour at 37°C. Sperm samples were isolated and purified from somatic cells. Briefly, the samples
335 were washed with PBS, and then incubated with SCLB (somatic cell lysis buffer, 0.1% SDS, 0.5%
336 TX-100 in Diethylpyrocarbonate water) for 1 hour. SCLB was rinsed off with 2 washes of PBS
337 and the somatic cell-free purified spermatozoa sample pelleted and used for RNA extraction.

338 ***Measurement of DDT metabolites:*** Liver tissues from CO, DDT and DDT-PB treated males,
339 collected within 24 h after last dose, were pooled (3 samples/group) and used to determine the
340 levels of DDT's main metabolites. Measurements were performed commercially by Pacific Rim
341 Labs, a fully accredited laboratory providing analysis of DDT and other persistent organic
342 pollutants. Briefly, samples were fortified with each of the six 13C-DDT isotopes and then
343 extracted with hexane. The extract was columned on Florisil and analyzed by GC-MS/MS. The
344 instrument was calibrated with a five-point calibration covering the range of 0.2-400 ng/g or mL.

345 ***Sperm Small RNA Sequencing:*** Total RNA was isolated from purified sperm using Qiagen's
346 miRNeasy extraction kit, according to the manufacturer's instructions. RNA integrity and quality
347 was examined by Bioanalyzer 2100 (Agilent Technologies). Small non-coding RNA transcript

libraries were constructed according to Illumina TrueSeq Small RNA Pre-Kit. After quality control, the library preparations were sequenced on an Illumina platform and reads generated. Raw data quality were checked using FastQC (v0.11.9), and adapter trimming on raw data were performed using Cutadapt (v3.5). Reads with low quality (quality score < 25, error rate > 10%) or reduced length after trimming (<15 bp) were removed before alignment. Single end trimmed reads was aligned against mouse reference genome downloaded from Ensembl GRCm38 release 101 using STAR (v2.7.9a). Small RNA tags were annotated with miRNA and t-RNA sequence fragments (tRFs) obtained from miRBase, GtRNAdb, Ref-seq, GenBank and Rfam databases using featureCounts (v2.0.3). DESeq2 R package (v1.36.0) was used for group wise statistical analysis. To allow for broad pattern identification of small RNAs, significance was set at p-value < 0.05, with a fold change threshold at >1.5.

Quantitative real time PCR validation (qRT-PCR): cDNA was synthesized from total RNA samples using the TaqMan™ Advanced cDNA Synthesis Kit (Applied Biosystems). PCR products were amplified from cDNA using TaqMan® Fast Advanced Master Mix and sequence-specific primers from TaqMan Assays (Applied Biosystems). Fold change was calculated from Ct values and the expression levels of specific miRNAs or genes were determined by normalizing these values with the fold change values for appropriate endogenous controls (miR-26a or *GAPDH*, respectively).

Embryonic RNA microinjections. To induce super-ovulation, female mice (*c57bl/6*) received intra-peritoneal injections of 5 IU of pregnant mare's serum gonadotropin (PMSG). About 48 hours after the PMSG injection, mice were injected with 5 IU of human chorionic gonadotropin (hCG). Super-ovulated females were mated with *c57bl/6* male mice. About 16 hours later,

370 fertilized eggs were harvested. Zygotes were injected with the RNA load from sperm of CO and
371 DDT-exposed males (sperm RNA isolated from 5 mice per group was pooled prior to injection).
372 Each zygote received 10 pL injection of the sperm RNA load (the amount of sperm RNA injected
373 is the equivalent to RNA from 10 sperm cells (7,18,19) or approximately 20-100 femtograms per
374 injection). Microinjections were confirmed by observing the swelling of the male pro-nucleus.
375 Injected zygotes were transferred into recipient female mice to produce offspring as described
376 before (17). Briefly, recipient females were mated with vasectomized males overnight and
377 identified by copulation plug before the zygote transfer. Each recipient female was implanted with
378 25-30 zygotes. Dams were housed in groups of two with free access to food and water. Female
379 offspring were used to study tumor growth or for tissue collection.
380 Another subset of zygotes was injected with synthetic miRNA-10b or scramble miR (at 20
381 femtograms per injection; *mir*Vana®, ThermoFisher) diluted in TE solution (10mM Tris-HCl,
382 pH7.4, 0.25 EDTA) or TE solution only (to control for microinjection). Synthetic miRNAs are
383 double- stranded RNA oligonucleotides that mimic a specific endogenous mature miRNA.
384 Injected zygotes were transferred into recipient female mice as described above for term delivery.
385 Female offspring were used to study tumor growth or for tissue collection.
386 A subset of the of zygotes injected with synthetic miRNA-10b or controls were cultured and
387 harvested at the blastocyst stage (E3.5) and used for RNA-seq analysis. Briefly, injected one-cell
388 zygotes were cultured in Advanced KSOM (Millipore, MR-101-D) at 37°C in 5% CO2 until
389 collected. Embryos at the blastocyst stage were collected at approximately 72 hours after miRNA
390 microinjection (~E3.5) and placed in M2 (Millipore, MR-015-D) and stored in -80°C.
391 ***Carcinogen-induced mammary tumorigenesis:*** Mammary tumors were induced in CO and DDT-
392 derived female offspring (CO, DDT, CO-RNA, DDT-RNA) by administration of MPA

(medroxyprogesterone acetate, 15 mg, s.c.) at 6 weeks of age, followed by three weekly doses of 1mg of 7,12-dimethylbenz[a]anthracene (DMBA) (Sigma, St. Louis, MO) dissolved in peanut oil by oral gavage. This established model of breast cancer has been used by us and others (8,37). Mice were examined for mammary tumors by palpation once per week, starting on week two after the last dose of DMBA and continue for up to 20 weeks after tumor detection. During follow-up, those animals in which tumor burden approximated 10% of total body weight were euthanized, as required by our institution. Tumor growth was measured using a caliper and the width and height of each tumor were recorded. Other end-points for data analysis were latency to tumor appearance and tumor incidence (percentage of animals with tumor in a given group). Histopathology of tumors was determined by a pathologist (S.G.). All tumors included in our analyses were classified as mammary carcinomas.

Syngeneic orthotopic tumor implantation: Syngeneic mammary tumors were induced in CO and DDT-derived female offspring [CO, DDT, CO-RNA, DDT-RNA, miR-10b and controls (scramble-miR or vehicle solution)]. Mouse EO771 breast cancer cells were cultured in complete medium [Dulbecco's Modified Eagle's Medium (DMEM) supplemented with 10% (v/v) FBS and 1% L-glutamine, at 37°C in 5% CO2 (v/v)] to 80% confluence, trypsinized, counted, checked for viability and re-suspended in PBS for injection into both 4th inguinal mammary glands. A total of $1x10^6$cells were injected into each of the 4th inguinal mammary gland fat pads. Tumor growth was monitored for ten weeks. During this period, those animals in which tumor burden approximated 10% of total body weight were euthanized, as required by our institution. Histopathology of tumors was determined by a pathologist (S.G.). All tumors included in our analyses were classified as mammary carcinomas.

415 ***Whole tissue RNA sequencing.*** Total RNA was isolated from snap frozen mouse tissues
416 (mammary tumors and embryos at the blastocyst stage) using Qiagen's RNeasy extraction kit,
417 according to the manufacturer's instructions. RNA integrity and quality was examined by
418 Bioanalyzer 2100 (Agilent Technologies). Transcript libraries were constructed using the TruSeq
419 mRNA Library Prep Kit (Illumina). After cluster generation, the library preparations were
420 sequenced on an Illumina platform and paired-end reads were generated. RNAseq raw data quality
421 was checked using FastQC (v0.11.09) and adapter trimming on raw data was performed using
422 Cutadapt (v3.5). Reads with low quality (quality score < 33, error rate > 10%) or reduced length
423 after trimming (<25 bp) were removed before alignment. We used the reference genome
424 downloaded from Ensembl GRCm38 release 101, and the reference index was built using Star
425 (v2.7.9a). Paired end trimmed read alignment and raw read count calculation was performed using
426 RSEM software (v1.3.1), and an additional bioinformatic workflow utilized Hisat2 v2.0.5 for
427 alignment to the GRCm38 genome and quantified to the Gencode vM25 transcriptome annotation
428 using Stringtie 2.2.1. For both workflows, differential expression analysis of two
429 conditions/groups was performed using the DESeq2 R package (v1.36.0), and visualized using the
430 Enhanced Volcano R package (v3.16). We considered the genes with q-value <0.1 to be
431 differentially expressed (DEG) in embryos and genes with a p-value <0.05 to be DEG in mammary
432 tumors to account for tissue heterogeneity. DEGs in mammary tumors were used as input for
433 Gene Set Enrichment Analysis (GSEA) (v4.2.3, Broad Institute). Both KEGG and HALLMARK
434 gene sets were selected for enrichment score calculation. DEGs in E3.5 embryos were used as
435 input for Gene Ontology (GO) functional characterization and pathway enrichment analysis. miR-
436 10b target prediction in E3.5 embryos was determined using TargetScan and miRBase.

Imaging mass cytometry (IMC): **Staining Procedures.** After baking for 2 hours at 60 °C, FFPE sections were dewaxed and rehydrated through a graded alcohol series. Heat-induced epitope retrieval was conducted in a steamer at 96 °C in antigen retrieval AR9 buffer for 30 min. After cooling, the sections were blocked with 3% BSA in PBS for 45 min at room temperature. Samples were incubated overnight at 4 °C with metal-conjugated antibody cocktails diluted in PBS/0.5% BSA (See **Table S4** for antibody list and dilutions). Samples were then washed twice with PBS/0.5% Tween and twice with PBS and exposed to 1:400 Ir-Intercalator (Fluidigm) for 30 min at RT for nuclei staining. The samples were rinsed in distilled water and air-dried before image acquisition. **Image Acquisition.** IMC data acquisition and visualization were performed as previously described(64,65). Briefly, stained and air-dried tumor slides were inserted into the ablation chamber of the Hyperion™ Imaging System (Fluidigm). The tissue was then scanned by a pulsed 200 Hz laser focused to a 1 μm spot and applied over a user-defined regions of interest (ROIs), ablating adjacent spots in 1 μm steps as the slide moves under the laser beam. Tissue from each ablation spot was vaporized and streamed by inert gas into the inductively coupled plasma ion source for analysis by the mass cytometer. Images of each mass channel were reconstructed by plotting the laser shot signals in the order in which they were recorded, line scan by line scan. Multi-channel images were overlaid for desired channel combinations in MCD™ Viewer v1.0.560.2 (Fluidigm).

Statistical analysis. Statistical analyses were performed using GraphPad Prism (GraphPad Software, San Diego, CA, USA). Normal probability plots were used to ascertain normality, which were confirmed by Anderson-Darling, D'Agostino-Pearson, Kolmogorov-Smirnov and Shapiro-Wilk tests. Where data failed the normality test, log transformation was performed prior to statistical analysis. Two-way ANOVA was used to analyze tumor growth curves (group, time –

with repeated measures) and IMC quantification data (group, tumor model) followed by post-hoc analysis using Fisher's LSD multiple comparison tests. Differences in tumor incidence (time to tumor appearance) were analyzed using Kaplan-Meier survival curves followed by the log-rank test. Differences in tumor latency (DMBA model only) and final tumor burden (% growth) were analyzed using unpaired t-test (for two groups) or Welch one-way ANOVA (for three groups), followed by Welch's t test. Gene and miRNA expression data was analyzed using one-way ANOVA, followed by Fisher's LSD multiple comparison test. Differences were considered statistically significant at $P < 0.05$. Unless indicated, *n* corresponds to the number of animals used in each experiment.

Acknowledgments: We thank the following Lombardi Cancer Center Shared Resources (SR) for their assistance: Animal Model SR, Histopathology & Tissue SR, Microscopy and Imaging SR and Genomics & Epigenomics SR. We also thank Mr. Chip Hawkins from the Johns Hopkins Transgenic Core Facility for technical support with embryos injections. We thank Dr. Sandra Jablonski and Dr. Louis Weiner for donating the murine EO771 cells.

Funding: This study was supported by the National Institutes of Health (ES031611 to Sonia de Assis and P30-CA51008; Lombardi Comprehensive Cancer Center Support Grant to Louis Weiner), the Georgetown Environmental Initiative (pilot fund to Sonia de Assis), and the American Cancer Society (RSG-16-203-01-NEC, Research Scholar Grant to Sonia de Assis).

Data availability: RNA-seq data (small RNAs and whole transcriptome) has been deposited in GEO (Gene Expression Omnibus) database under accession codes GSE221649 and GSE222357.

Author contributions: S.D.A. conceived the study, oversaw the research and wrote the manuscript; R.S.D.C. conceived the study, supervised the animal work and tissue collection, performed molecular analysis and wrote the manuscript; O.D., E.C., A.N., A.K.G. and X.Z. assisted with animal studies, processed tissues and/or helped perform molecular analysis; I.P. performed IMC analysis, M.I.C. assisted with animal studies; S.G. performed histopathological classification of tumors; L.J., M.S. and M.M. performed RNA-seq data and enrichment analysis; K.M. assisted with statistical analysis.

References

1. Hitchins MP. Constitutional epimutation as a mechanism for cancer causality and heritability? Nat Rev Cancer **2015**;15:625-34
2. Chen Q YW, Duan W. Epigenetic inheritance of acquired traits through sperm RNAs and sperm RNA modifications. Nature Reviews Genetics **2016**;17
3. da Cruz RS, Chen E, Smith M, Bates J, de Assis S. Diet and Transgenerational Epigenetic Inheritance of Breast Cancer: The Role of the Paternal Germline. Front Nutr **2020**;7:93
4. OJ R. Daddy issues: paternal effects on phenotype. Cell **2012**;151:702-8
5. MK JRS. Environmental epigenomics and disease susceptibility. Nature Review Genetics **2007**;8:253-62
6. de Assis S WA, Cruz MI, Laja O, Tian Y, Zhang B, Wang Y, Huang T, Hilakivi-Clarke L. High-fat or ethinyl-oestradiol intake during pregnancy increases mammary cancer risk in several generations of offspring. Nature Communications **2012**;3
7. Gapp K JA, Sarkies P, Bohacek J, Pelzcar P, Prados J, Farinelli L, Miska E, Mansuy IM. Implication of sperm RNAs in transgenerational inheritence of the effects of early trauma in mice. Nature Neuroscience **2014**;17:667-9
8. Fontelles CC, Carney E, Clarke J, Nguyen NM, Yin C, Jin L*, et al.* Paternal overweight is associated with increased breast cancer risk in daughters in a mouse model. Sci Rep **2016**;6:28602
9. Fontelles CC, Guido LN, Rosim MP, Andrade Fde O, Jin L, Inchauspe J*, et al.* Paternal programming of breast cancer risk in daughters in a rat model: opposing effects of animal- and plant-based high-fat diets. Breast Cancer Res **2016**;18:71
10. da Cruz RS, Carney EJ, Clarke J, Cao H, Cruz MI, Benitez C*, et al.* Paternal malnutrition programs breast cancer risk and tumor metabolism in offspring. Breast Cancer Res **2018**;20
11. da Cruz RS, Clarke J, Curi AC, Al-Yawar A, Jin L, Baird A*, et al.* Parental obesity programs pancreatic cancer development in offspring. Endocr Relat Cancer **2019**
12. Ng SF LR, Barres R, Owens JA, Morris MJ. Chronic high-fat diet in fathers programs β-cell dysfunction in female rat offspring. Nature **2010**;467:963-6
13. Caronne BR FL, Habib N, Shea JM, Hart CE, Li R, Bock C, Li C, Gu H, Zamore PD, Meissner A, Weng Z, Hofmann HA, Friedman N, Rando OJ. Paternally induced transgenerational environment reprogramming of metabolic gene expression in mammals. Cell **2010**;143:1084-96
14. Guido LN, Fontelles CC, Rosim MP, Pires VC, Cozzolino SM, Castro IA*, et al.* Paternal selenium deficiency but not supplementation during preconception alters mammary gland development and 7,12-dimethylbenz[a]anthracene-induced mammary carcinogenesis in female rat offspring. Int J Cancer **2016**;139:1873-82
15. Chen Q, Yan M, Cao Z, Li X, Zhang Y, Shi J*, et al.* Sperm tsRNAs contribute to intergenerational inheritance of an acquired metabolic disorder. Science **2015**
16. Sharma U, Conine CC, Shea JM, Boskovic A, Derr AG, Bing XY*, et al.* Biogenesis and function of tRNA fragments during sperm maturation and fertilization in mammals. Science **2015**
17. Rodgers AB MC, Leu NA, Bale TL. Transgenerational epigenetic programming via sperm microRNA recapitulates effects of paternal stress. Proceedings of the National

Academy of Sciences of the United States of America **2015**;112:13699-704

18. Chen Q YM, Cao Z, Li X, Zhang Y, Shi J, Feng GH, Peng H, Zhang X, Zhang Y, Qian J, Duan E, Zhai Q, Zhou Q. Sperm tsRNAs contribute to intergenerational inheritance of an acquired metabolic disorder. Science **2016**;351:397-400
19. Wang Y, Chen ZP, Hu H, Lei J, Zhou Z, Yao B*, et al.* Sperm microRNAs confer depression susceptibility to offspring. Sci Adv **2021**;7
20. Cohn BA LMM, Krigbaum NY, Yeh G, Park JS, Zimmermann L, Cirillo PM. DDT Exposure in Utero and Breast Cancer. Journal of Clinical Endocrinology and Metabolism **2015**;100:2865-72
21. Cohn BA, Wolff MS, Cirillo PM, Sholtz RI. DDT and breast cancer in young women: new data on the significance of age at exposure. Environ Health Perspect **2007**;115:1406-14
22. Zahm SH, Ward MH. Pesticides and childhood cancer. Environ Health Perspect **1998**;106 Suppl 3:893-908
23. Greenop KR PS, Bailey HD, Fritschi L, Attia J, Scott RJ, Glass DC, de Klerk NH, Alvaro F, Armstrong BK, Milne E. Exposure to pesticides and the risk of childhood brain tumors. Cancer Causes & Control **2013**;24:1269-78
24. Bailey H FL, Infante-Rivard C, Glass DC, Miligi L, Dockerty JD, Lightfoot T, Clavel J, Roman E, Spector LG, Kaatsch P, Metayer C, Magnani C, Milne E, Polychronopoulou S, Simpson J, Rudant J, Sidi V, Rondelli R, Orsi L, Kang A, Petridou E, Schüz J. Parental occupational pesticide exposure and the risk of childhood leukemia in the offspring: Findings from the Childhood Leukemia International Consortium. International Journal of Cancer **2014**;135:2157-72
25. Park AS, Ritz B, Yu F, Cockburn M, Heck JE. Prenatal pesticide exposure and childhood leukemia - A California statewide case-control study. Int J Hyg Environ Health **2020**;226:113486
26. Lombardi C, Thompson S, Ritz B, Cockburn M, Heck JE. Residential proximity to pesticide application as a risk factor for childhood central nervous system tumors. Environ Res **2021**;197:111078
27. Gunier RB, Kang A, Hammond SK, Reinier K, Lea CS, Chang JS*, et al.* A task-based assessment of parental occupational exposure to pesticides and childhood acute lymphoblastic leukemia. Environ Res **2017**;156:57-62
28. Van Maele-Fabry G, Gamet-Payrastre L, Lison D. Residential exposure to pesticides as risk factor for childhood and young adult brain tumors: A systematic review and meta-analysis. Environ Int **2017**;106:69-90
29. Whitehead TP, Metayer C, Wiemels JL, Singer AW, Miller MD. Childhood Leukemia and Primary Prevention. Curr Probl Pediatr Adolesc Health Care **2016**;46:317-52
30. Cohn BA, Cirillo PM, Terry MB. DDT and Breast Cancer: Prospective Study of Induction Time and Susceptibility Windows. J Natl Cancer Inst **2019**
31. Knower KC TS, Leung YK, Ho SM, Clyne CD. Endocrine disruption of the epigenome: a breast cancer link. Endorcrine Related Cancer **2014**;21:T33-55
32. Kabasenche WP, Skinner MK. DDT, epigenetic harm, and transgenerational environmental justice. Environ Health **2014**;13:62
33. SE MMF. Endocrine disruptors and the breast: early life effects and later life disease. Journal of Mammargy Gland Biology and Neoplasia **2013**;18:43-61
34. Kuiper GG, Lemmen JG, Carlsson B, Corton JC, Safe SH, van der Saag PT*, et al.*

Interaction of estrogenic chemicals and phytoestrogens with estrogen receptor beta. Endocrinology **1998**;139:4252-63

35. Ruiz D, Becerra M, Jagai JS, Ard K, Sargis RM. Disparities in Environmental Exposures to Endocrine-Disrupting Chemicals and Diabetes Risk in Vulnerable Populations. Diabetes Care **2018**;41:193-205

36. Daniels SI, Chambers JC, Sanchez SS, La Merrill MA, Hubbard AE, Macherone A*, et al.* Elevated Levels of Organochlorine Pesticides in South Asian Immigrants Are Associated With an Increased Risk of Diabetes. J Endocr Soc **2018**;2:832-41

37. Apostoli AJ, Skelhorne-Gross GE, Rubino RE, Peterson NT, Di Lena MA, Schneider MM*, et al.* Loss of PPARγ expression in mammary secretory epithelial cells creates a pro-breast tumorigenic environment. Int J Cancer **2014**;134:1055-66

38. Schuster A, Skinner MK, Yan W. Ancestral vinclozolin exposure alters the epigenetic transgenerational inheritance of sperm small noncoding RNAs. Environ Epigenet **2016**;2

39. Sharma U CC, Shea JM, Boskovic A, Derr AG, Bing XY, Belleannee C, Kucukural A, Serra RW, Sun F, Song L, Caronne BR, Ricci EP, Li XZ, Fauquier L, Moore MJ, Sullivan R, Mello CC, Garber M, Rando OJ. Biogenesis and function of tRNA fragments during sperm maturation and fertilization in mammals. Science **2016**;351:391-6

40. Sharma U, Sun F, Conine CC, Reichholf B, Kukreja S, Herzog VA*, et al.* Small RNAs Are Trafficked from the Epididymis to Developing Mammalian Sperm. Dev Cell **2018**;46:481-94 e6

41. Davies JE, Edmundson WF, Carter CH, Barquet A. Effect of anticonvulsant drugs on dicophane (D.D.T.) residues in man. Lancet **1969**;2:7-9

42. Kwalick DS. Anticonvulsants and DDT residues. JAMA **1971**;215:120-1

43. Alary JG, Guay P, Brodeur J. Effect of phenobarbital pretreatment on the metabolism of DDT in the rat and the bovine. Toxicol Appl Pharmacol **1971**;18:457-68

44. Lambert G, Brodeur J. [Influence of various enzyme inductors and combinations of inductors on DDT residue elimination in rats]. Rev Can Biol **1976**;35:33-41

45. Lambert G, Brodeur J. [The effect of pretreatment with enzyme inducers on the acute toxicity of DDT (1, 1-bis-(p-chlorophenyl)-2,2,2-trichloroethane) in rats]. Rev Can Biol **1975**;34:121-9

46. Hudson K, Cross N, Jordan-Mahy N, Leyland R. The Extrinsic and Intrinsic Roles of PD-L1 and Its Receptor PD-1: Implications for Immunotherapy Treatment. Front Immunol **2020**;11:568931

47. Belleannee C, Calvo E, Caballero J, Sullivan R. Epididymosomes convey different repertoires of microRNAs throughout the bovine epididymis. Biol Reprod **2013**;89:30

48. Gapp K, Miska EA. tRNA fragments: novel players in intergenerational inheritance. Cell Res **2016**;26:395-6

49. Chen Y, Kim J, Yang S, Wang H, Wu CJ, Sugimoto H*, et al.* Type I collagen deletion in alphaSMA(+) myofibroblasts augments immune suppression and accelerates progression of pancreatic cancer. Cancer Cell **2021**;39:548-65 e6

50. Tehler D, Hoyland-Kroghsbo NM, Lund AH. The miR-10 microRNA precursor family. RNA Biol **2011**;8:728-34

51. Cropley JE, Eaton SA, Aiken A, Young PE, Giannoulatou E, Ho JWK*, et al.* Male-lineage transmission of an acquired metabolic phenotype induced by grand-paternal obesity. Mol Metab **2016**;5:699-708

52. Schuster A, Tang C, Xie Y, Ortogero N, Yuan S, Yan W. SpermBase: A Database for

Sperm-Borne RNA Contents. Biol Reprod **2016**;95:99

53. Donkin I VS, Ingerselv LR, Qian K, Mechta M, Nordkap L, Mortensen B, Appel EV, Jørgensen N, Kristiansen VB, Hansen T, Workman CT, Zierath JR, Barrès R. Obesity and Bariatric Surgery Drive Epigenetic Variation of Spermatazoa in Humans. Cell Metabolism **2016**;23:369-78

54. Skinner MK, Ben Maamar M, Sadler-Riggleman I, Beck D, Nilsson E, McBirney M*, et al.* Alterations in sperm DNA methylation, non-coding RNA and histone retention associate with DDT-induced epigenetic transgenerational inheritance of disease. Epigenetics Chromatin **2018**;11:8

55. Nicolella HD, de Assis S. Epigenetic Inheritance: Intergenerational Effects of Pesticides and Other Endocrine Disruptors on Cancer Development. Int J Mol Sci **2022**;23

56. Montjean D, Neyroud AS, Yefimova MG, Benkhalifa M, Cabry R, Ravel C. Impact of Endocrine Disruptors upon Non-Genetic Inheritance. Int J Mol Sci **2022**;23

57. Denny Vågerö PRP, Vanda Aronsson & Gerard J. van den Berg Paternal grandfather's access to food predicts all-cause and cancer mortality in grandsons. Nature Communications **2018**;9: 5124

58. CDC. The Fourth National Report on Human Exposure to Environmental Chemicals, 2009, (the Fourth Report). **2009**;Updated Tables-January 2019

59. Kortenkamp A, Faust M. Combined exposures to anti-androgenic chemicals: steps towards cumulative risk assessment. Int J Androl **2010**;33:463-74

60. Stoker TE, Cooper RL, Lambright CS, Wilson VS, Furr J, Gray LE. In vivo and in vitro anti-androgenic effects of DE-71, a commercial polybrominated diphenyl ether (PBDE) mixture. Toxicol Appl Pharmacol **2005**;207:78-88

61. Kharlyngdoh JB, Pradhan A, Olsson PE. Androgen receptor modulation following combination exposure to brominated flame-retardants. Sci Rep **2018**;8:4843

62. James ER, Carrell DT, Aston KI, Jenkins TG, Yeste M, Salas-Huetos A. The Role of the Epididymis and the Contribution of Epididymosomes to Mammalian Reproduction. Int J Mol Sci **2020**;21

63. La Merrill M KE, Moshier E, Lindtner C, La Frano MR, Newman JW, Buettner C. Perinatal exposure of mice to the pesticide DDT impairs energy expenditure and metabolism in adult female offspring. PLoS One **2014**;9

64. Chang Q, Ornatsky OI, Siddiqui I, Straus R, Baranov VI, Hedley DW. Biodistribution of cisplatin revealed by imaging mass cytometry identifies extensive collagen binding in tumor and normal tissues. Sci Rep **2016**;6:36641

65. Peran I, Dakshanamurthy S, McCoy MD, Mavropoulos A, Allo B, Sebastian A*, et al.* Cadherin 11 Promotes Immunosuppression and Extracellular Matrix Deposition to Support Growth of Pancreatic Tumors and Resistance to Gemcitabine in Mice. Gastroenterology **2021**;160:1359-72 e13

Figure Legends

Figure 1. Paternal exposure to DDT leads to enhanced breast tumor growth in offspring.
(a) Schematic representation of the experimental design: Eight week-old male mice were treated with a vehicle-control (CO) or a DDT solution (1.7 mg/kg) via oral gave for 17 days. CO and DDT males were subsequently mated to unexposed females to generate offspring.

(b-e) Carcinogen-induced mammary tumorigenesis CO and DDT female offspring: (b) Mammary tumor volume (n=14), (c) tumor burden (percentage growth, n=14), (d) tumor incidence (n=25) and (e) tumor latency (n=12-15).

(f-g) Orthotopic (EO771 cells) mammary tumorigenesis in CO and DDT female offspring: (f) Mammary tumor volume (n=9-11) and (g) tumor burden (percentage growth, n=8-10).

Tumor incidence is shown as percentage of animals with tumors; All other data are shown as mean (horizontal bars in scatter plots) or mean± SEM (tumor growth curves). Tumor burden data does not include tumors with fewer than two measurements. Tumor latency includes both measurable and non-measurable tumors. Tumor volume curves were analyzed using two-away ANOVA (group, time – with repeated measures). Differences in tumor incidence were analyzed using Kaplan-Meier survival curves followed by the log-rank test. Differences in final tumor burden (% growth) and tumor latency were analyzed using unpaired t-test. P values are displayed in each figure panel.

Figure 2. Sperm RNAs contribute to DDT-induced paternal transmission of breast cancer predisposition to offspring.
(a) Schematic representation of the experimental design: Normal mouse embryos at the zygote stage were injected with the RNA load from sperm of CO or DDT-exposed males. Injected zygotes were transferred into recipient female mice to produce offspring.

(b-e) Carcinogen-induced mammary tumorigenesis in CO-RNA and DDT-RNA female offspring: (b) Mammary tumor volume (n=6-10), (c) tumor burden (percentage growth, n=6-10), (d) tumor incidence(n=7-10) and (e) tumor latency (n=6-10).

(f-g) Orthotopic (EO771 cells) mammary tumorigenesis CO-RNA and DDT-RNA female offspring: (f) Mammary tumor volume (n=5-8) and (g) tumor burden (percentage growth, n=5-8).

Tumor incidence is shown as percentage of animals with tumors; All other data are shown as mean (scatter plots) or mean± SEM (tumor growth curves). Tumor burden data does not include tumors with fewer than two measurements. Tumor latency includes both measurable and non-measurable tumors. Tumor volume curves were analyzed using two-away ANOVA (group, time – with repeated measures). Differences in tumor incidence were analyzed using Kaplan-Meier survival curves followed by the log-rank test. Differences in final tumor burden (% growth) and tumor latency were analyzed using unpaired t-test. P values are displayed in each figure panel.

Figure 3. DDT exposure reprograms the sperm small non-coding RNA load.
(a) Schematic representation of the experimental design: Eight week-old male mice were treated orally with a vehicle-control (CO) or a DDT solution (1.7 mg/kg) for 17 days. RNA extracted from sperm of CO and DDT-exposed males was analyzed via RNA-seq.

(b) Small RNA subtype distribution (percentage of raw reads) and (c) heat-map showing differentially expressed miRNAs in sperm of CO and DDT-exposed males (n=9).

(d-e) Proportional abundance of differentially expressed miRNAs (DESeq2 normalized counts) in sperm of (d) CO and (e) DDT-exposed males (n=9).

Figure 4. Treatment with the hepatic enzyme inducer, phenobarbital, leads to reduction of DDT metabolites and normalization of sperm miRNA-10b levels in DDT-exposed males.
(a) Schematic representation of the experimental design: Eight week-old male mice were treated orally with a vehicle-control (CO) or a DDT solution (1.7 mg/kg) with or without i.p. injection of phenobarbital (PB, 20mg/kg) treatment.

(b) Expression levels of *Cyp2B10*, assessed by q-PCR, in liver tissues of CO and DDT-exposed male mice treated with PB or vehicle injection (n=4-5).

(c) Levels of DDT metabolites in liver tissues of CO and DDT-exposed male mice treated with PB or vehicle injection (n=3 pools).

(d) miRNA expression levels (DESeq2 normalized counts), assessed by RNA-seq, in sperm of CO and DDT-exposed male mice treated with PB or vehicle injection (n=5-9).

(e) Expression levels of miRNA-10b, assessed by q-PCR, in sperm of CO and DDT-exposed male mice treated with PB or vehicle injection (n=8-16).

Expression levels of *Cyp2B10* and miRNA-10b are relative to GAPDH and miR-26a, respectively. Data are shown as mean (horizontal bars in scatter plots) or mean± SEM (bar graphs). ns, non-significant, *$p<0.05$, **$p<0.01$, ***$p<0.001$, ****$p<0.0001$. Expression data was analyzed using one-way ANOVA.

Figure 5. miRNA-10b embryonic injection recapitulates tumor phenotypes observed in offspring of DDT-exposed fathers.
(a) Schematic representation of the experimental design: Normal mouse embryos at the zygote stage were injected with synthetic miRNA-10b, scramble miRNA (miR-Src) or vehicle-control (CO-veh). Injected zygotes were culture to the blastocyst stage or transferred into recipient female mice to produce offspring.

(b-c) Orthotopic (EO771 cells) mammary tumorigenesis in controls and miR-10b female offspring: (b) Mammary tumor volume (n=3-10) and (c) tumor burden (percentage growth, n=3-10).

(d) Volcano plot showing differentially expressed genes (DEG) in miR-10b-injected E3.5 embryos (n=3 pools).

(e) Functional annotation of DEG in miR-10b-injected E3.5 embryos.

Data are shown as mean (horizontal bars in scatter plots) or mean± SEM (tumor growth curves). Tumor volume curves were analyzed using two-away ANOVA (group, time – with repeated measures). Differences in final tumor burden (% growth) were analyzed using one-way ANOVA. P values are displayed in each figure panel.

Figure 6. Tumors of DDT-derived offspring have distinct signaling programs and alterations in the stromal and immune compartments.
(a) GSEA analysis of DEG in mammary tumors of DDT-derived offspring (DDT, DDT-RNA and miRNA-10b, n=3), showing significantly down-regulated pathways: Epithelial Mesenchymal Transition, Interferon γ Response, and Allograft Rejection.

(b) IMC staining for collagen type I (green), E-cadherin (red), DNA (blue, iridium intercalator) and quantification of collagen type I from IMC data in orthotopic (EO771 cells, n=9-12) and carcinogen-induced mammary tumors of DDT-derived offspring (n=6). Scale bar equals to 200 μm.

(c) IMC staining for α-SMA (cyan), E-cadherin (red), DNA (blue, iridium intercalator) and quantification of α-SMA from IMC data in in orthotopic (EO771 cells, n=9-12) and carcinogen-induced mammary tumors of DDT-derived offspring (n=6). Scale bar equals to 200 μm.

(d) IMC staining for PD-L1(white), DNA (blue, iridium intercalator) and quantification of PD-L1 from IMC data in orthotopic (EO771 cells, n=9-12) and carcinogen-induced mammary tumors of DDT-derived offspring (n=6). Scale bar equals to 200 μm.

Horizontal bars in scatter plots represent the mean in b-d. ns, non-significant, *$p<0.05$, **$p<0.01$, ****$p<0.0001$. IMC quantification data was analyzed using two-way ANOVA(group, tumor model).

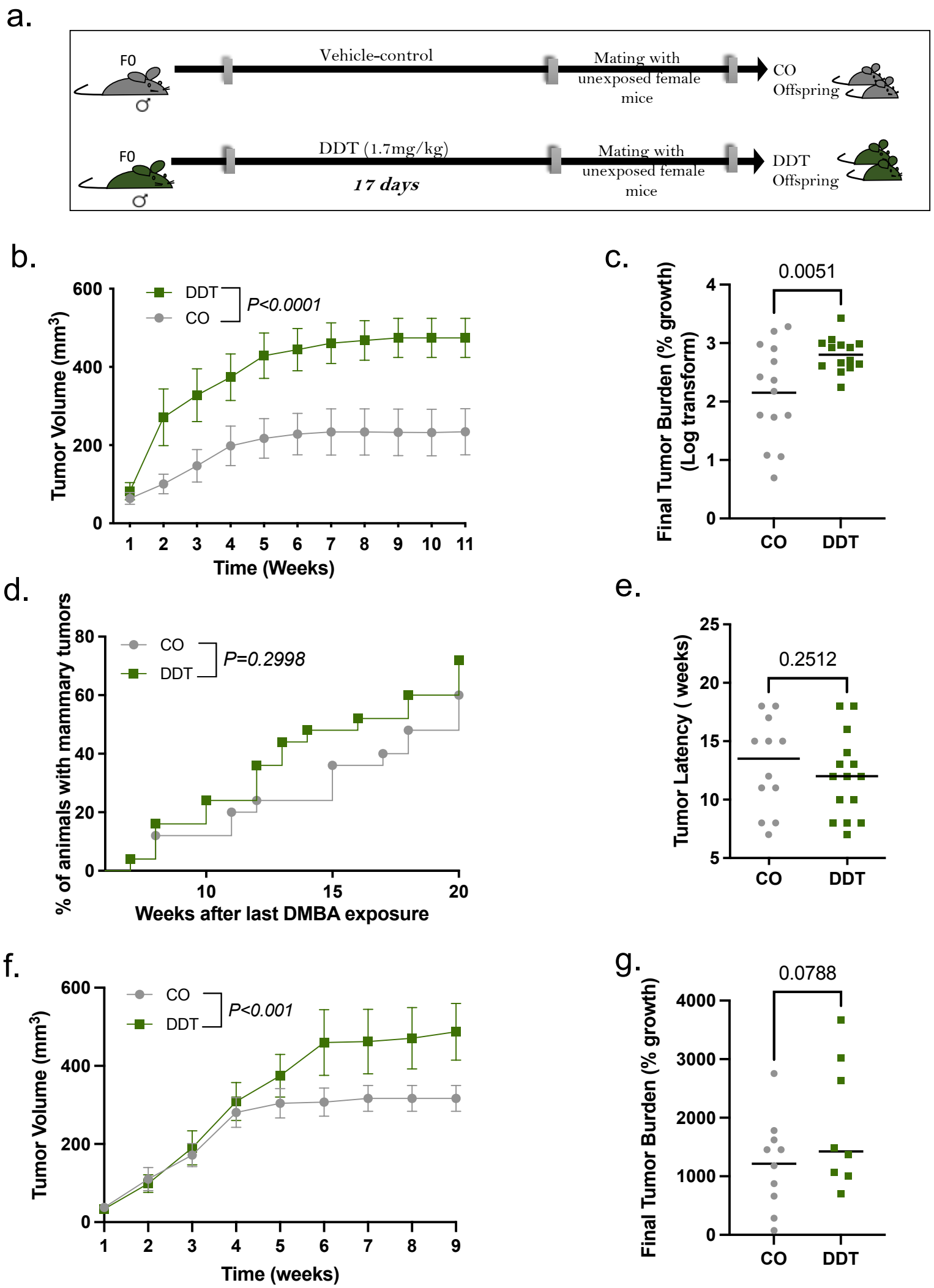
a.
F0
Vehicle-control
Mating with unexposed female mice
CO Offspring
F0
DDT (1.7mg/kg)
17 days
Mating with unexposed female mice
DDT Offspring
b.
DDT
CO
P<0.0001
Tumor Volume (mm3)
Time (Weeks)
c.
0.0051
Final Tumor Burden (% growth) (Log transform)
CO
DDT
d.
CO
DDT
P=0.2998
% of animals with mammary tumors
Weeks after last DMBA exposure
e.
0.2512
Tumor Latency (weeks)
CO
DDT
f.
CO
DDT
P<0.001
Tumor Volume (mm3)
Time (weeks)
g.
0.0788
Final Tumor Burden (% growth)
CO
DDT

Figure 1

a.

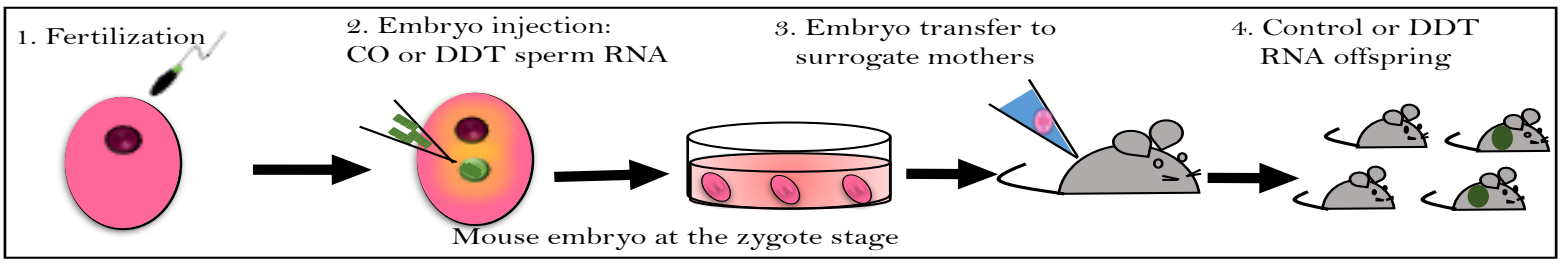

b.

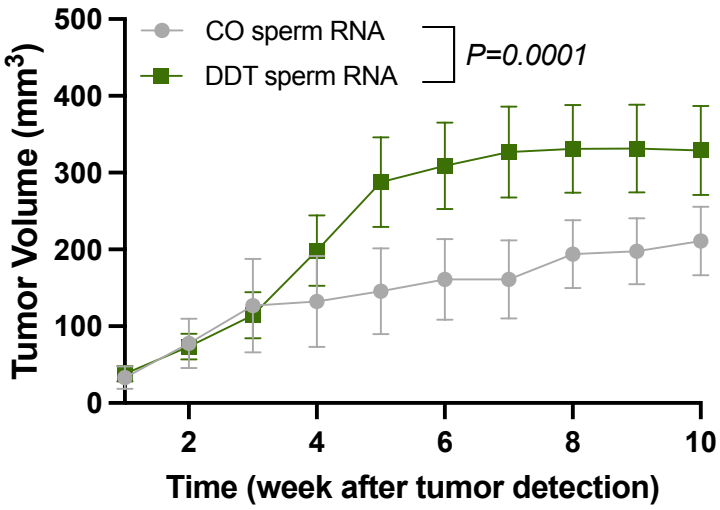

c.

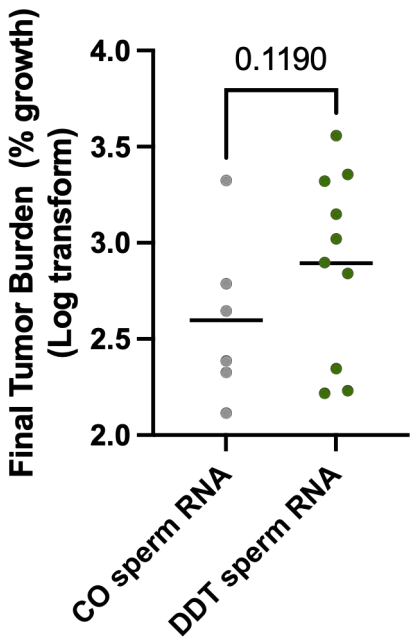

d.

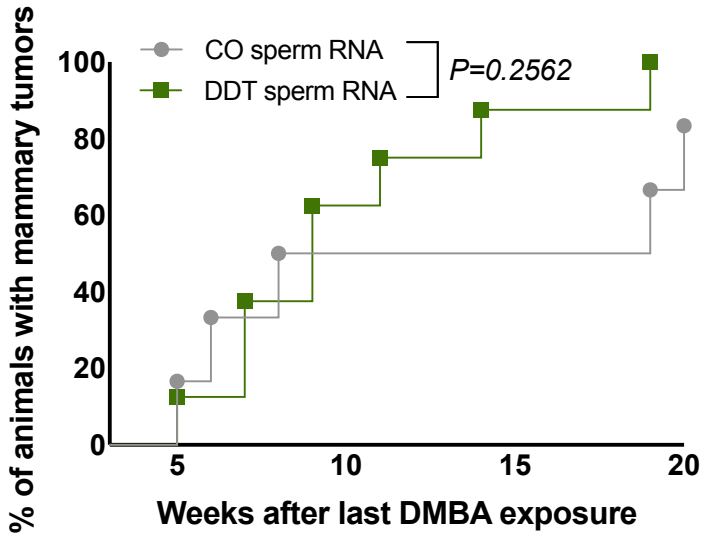

e.

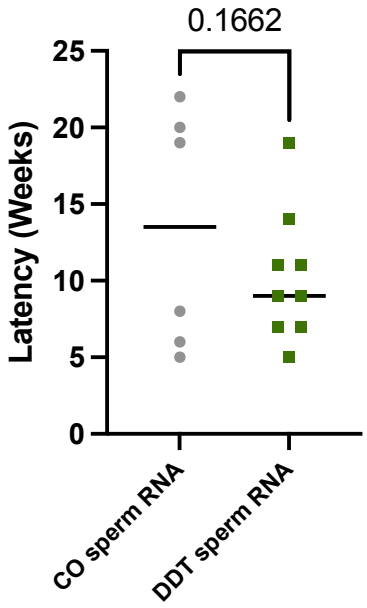

f.

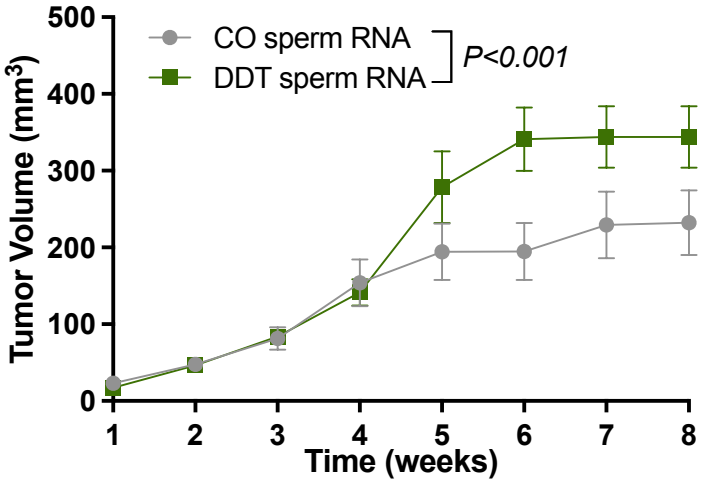

g.

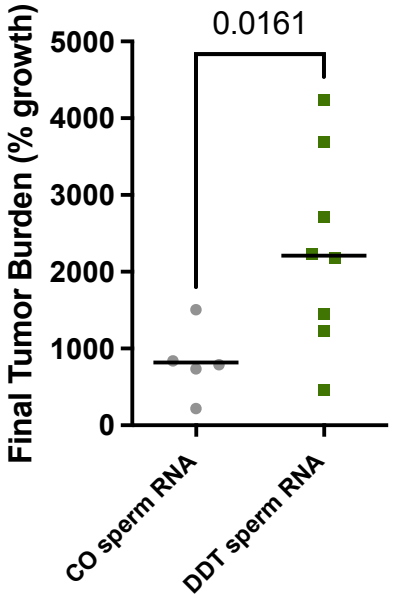

Figure 2

a.

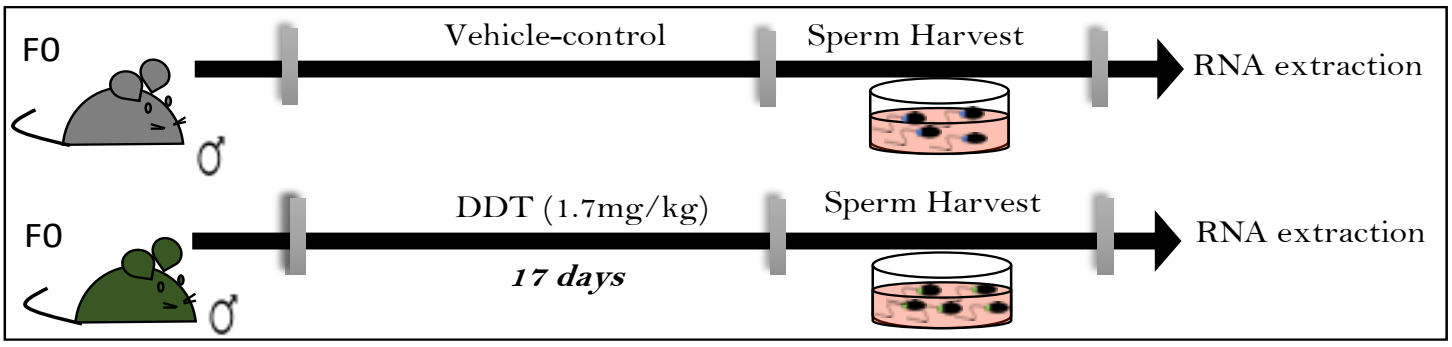

b.

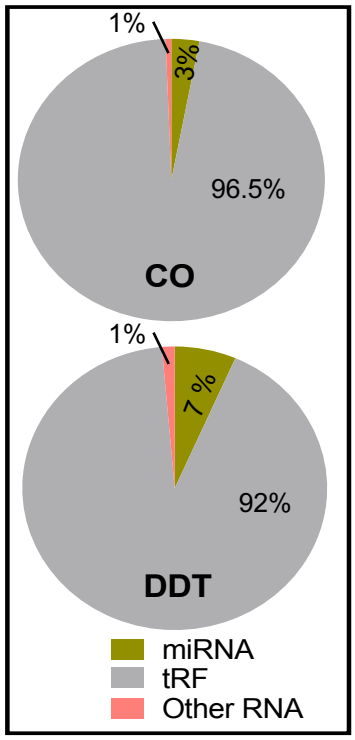

c.

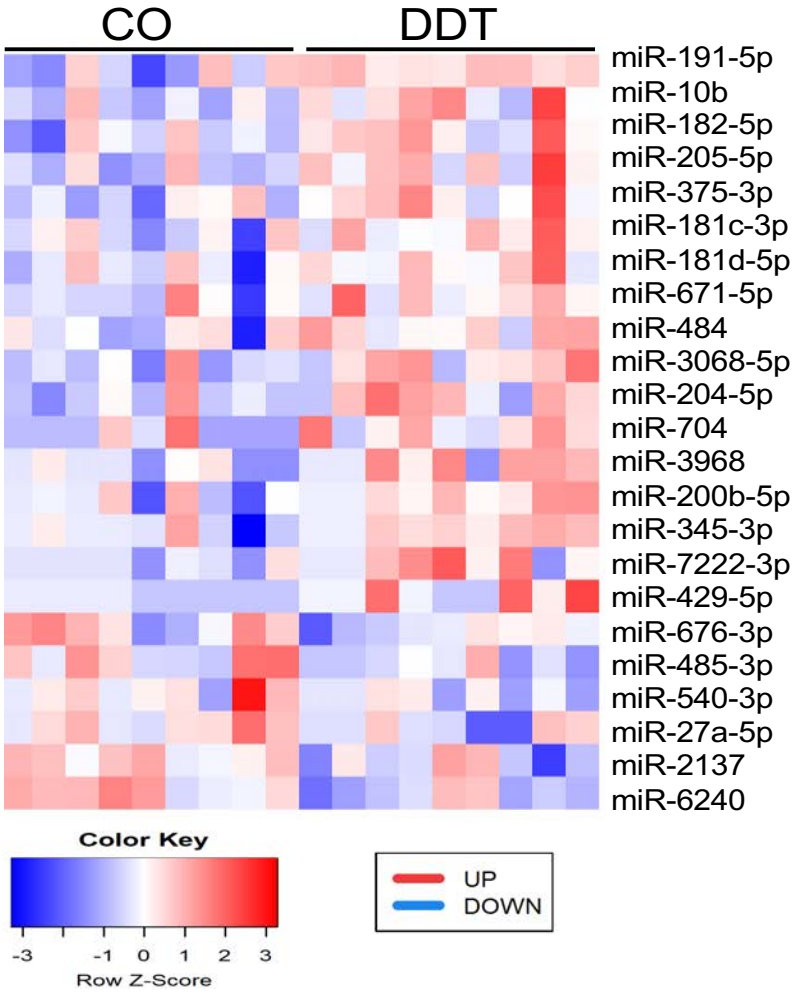

d.

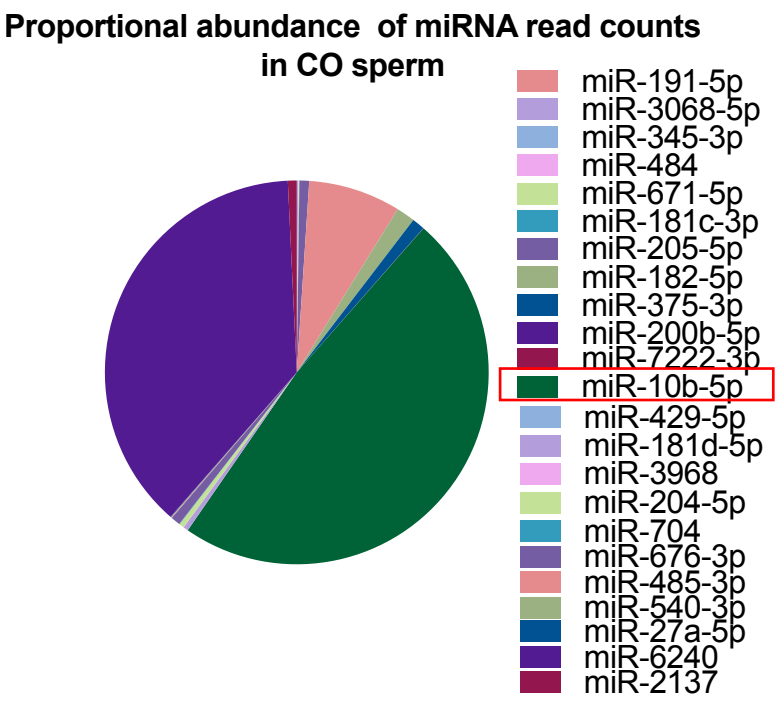

e.

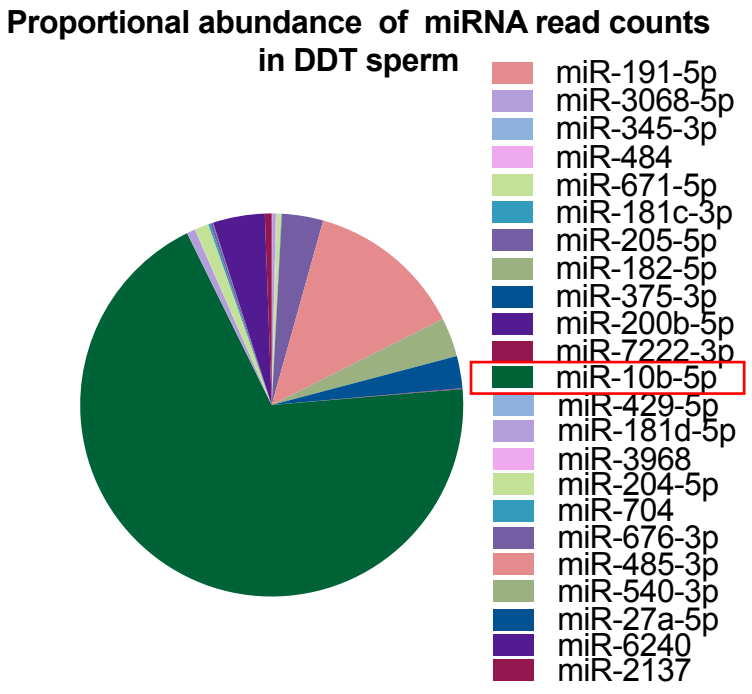

Figure 3

a.

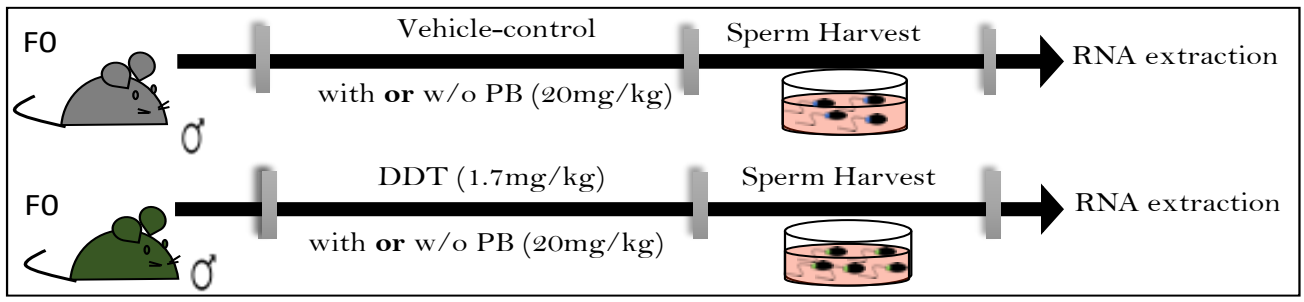

b.

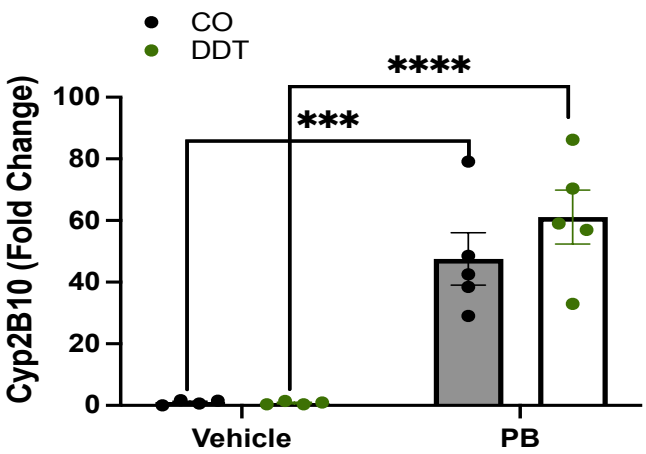

c.

Levels of DDT metabolites in liver (ng/g)

Analyte	QC Blank (Detection limit)	Vehicle-control	DDT	DDT+PB
o,p'-DDE	ND (0.2)	ND	ND	ND
p,p-DDE	ND (0.2)	ND	**0.55**	ND
o,p'-DDD	ND (0.04)	ND	ND	ND
p,p-DDD	ND (0.04)	ND	**0.28**	**0.06**

d.

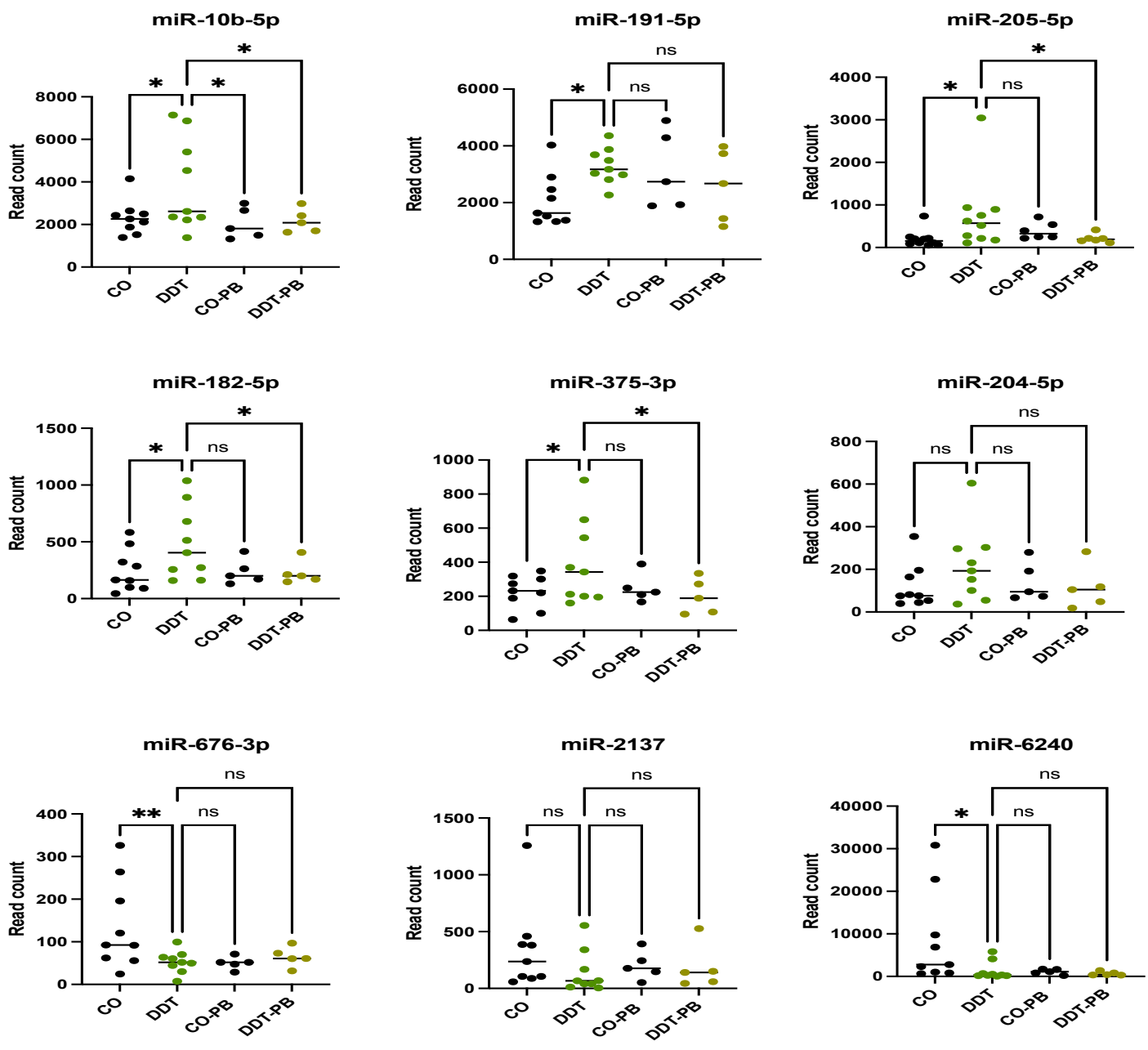

e.

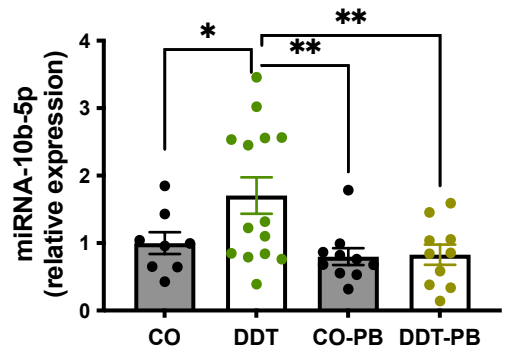

Figure 4

a.

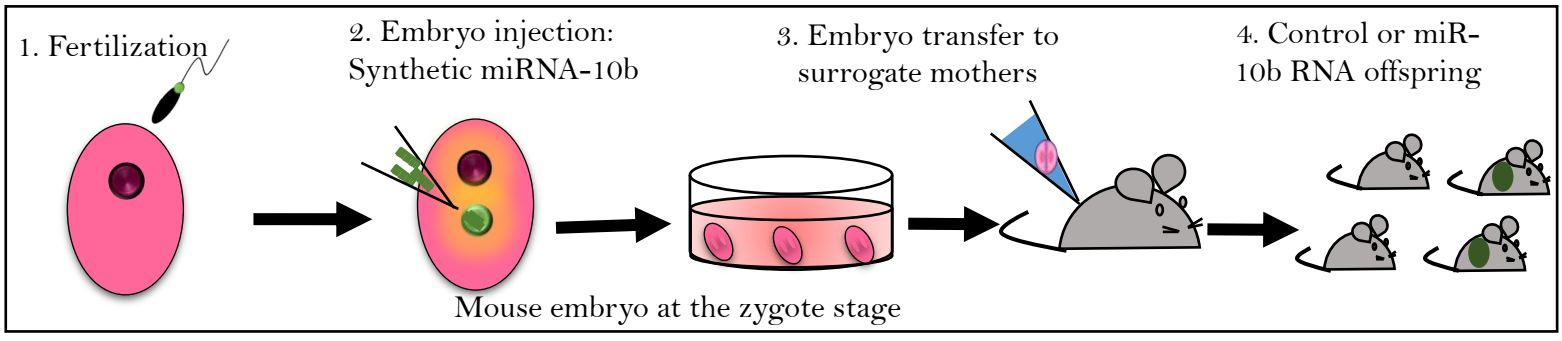

b.

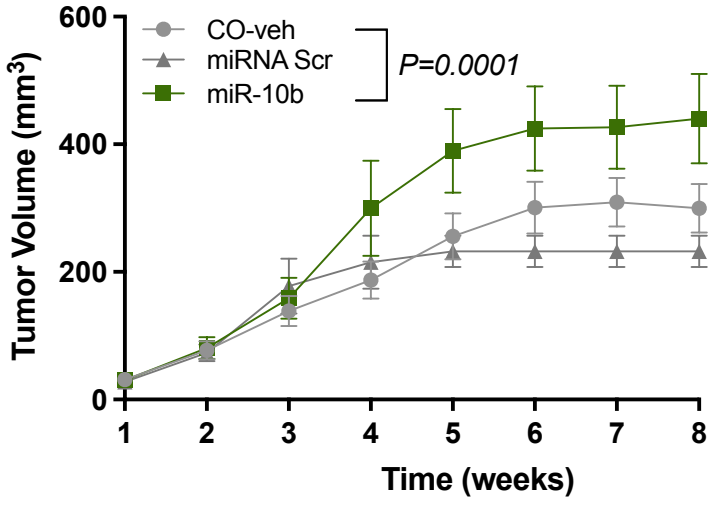

c.

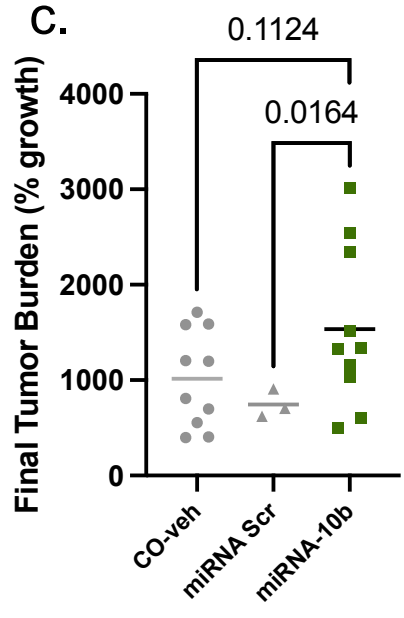

d.

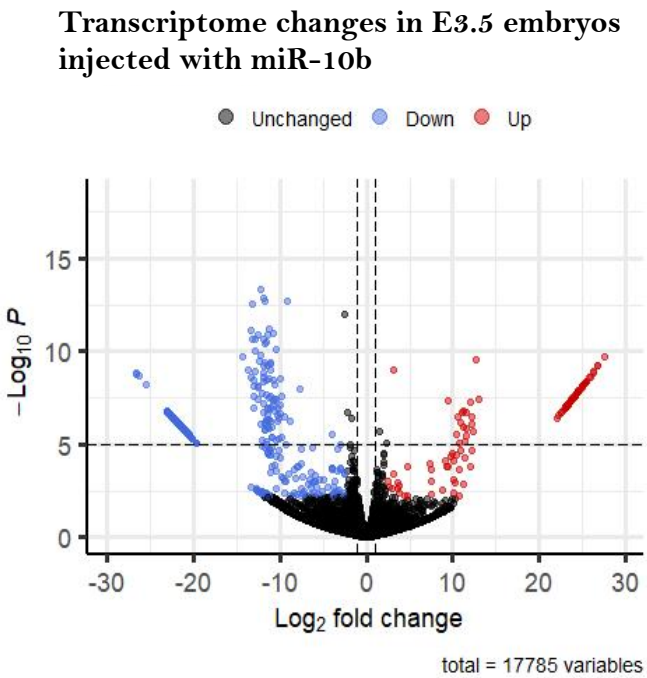

e.

Functional Annotation of DEGs in miR-10b injected embryos (Top GO and MP categories)

Term ID	*Description*	*Adjusted P value*
GO:0009888	Tissue development	0.0048
GO:0045595	Regulation of cell differentiation	0.0058
GO:0032501	Multicellular organismal process	0.0063
GO:0048468	Cell development	0.0063
GO:0048513	Animal organ development	0.0063
GO:0060429	Epithelium development	0.0063
GO:0007275	Multicellular organism development	0.007
GO:0009653	Anatomical structure morphogenesis	0.007
GO:0009790	Embryo development	0.007
GO:0030154	Cell differentiation	0.007
MP:0001764	Abnormal homeostasis	0.00014
MP:0002396	Abnormal hematopoietic system morphology/development	0.00014
MP:0005376	Homeostasis/metabolism phenotype	0.00014
MP:0005397	Hematopoietic system phenotype	0.00014
MP:0000516	Abnormal renal/urinary system morphology	0.00019
MP:0000685	Abnormal immune system morphology	0.00026
MP:0013656	Abnormal hematopoietic cell morphology	0.00076
MP:0005387	Immune system phenotype	0.00093
MP:0012382	Abnormal blood cell physiology	0.0018
MP:0002421	Abnormal cell-mediated immunity	0.0034

Figure 5

a.

Epithelial to Mesenchymal Transition | Interferon Gamma Response | Allograft Rejection

DDT vs. CO

HALLMARK_EPITHELIAL_MESENCHYMAL_TRANSITION — NES: 1.90, p-value: 0.0, FDR : 0.0

HALLMARK_INTERFERON_GAMMA_RESPONSE — NES: 1.38, p-value: 0.0, FDR : 0.017

Enrichment plot: HALLMARK_ALLOGRAFT_REJECTION — NES: 1.38, p-value: 0.014, FDR: 0.08

DDT-RNA vs. CO-RNA

HALLMARK_EPITHELIAL_MESENCHYMAL_TRANSITION — NES: 2.87, p-value: 0.0, FDR: 0.0

HALLMARK_INTERFERON_GAMMA_RESPONSE — NES: 2.12, p-value: 0.0, FDR: 0.0

Enrichment plot: HALLMARK_ALLOGRAFT_REJECTION — NES: 2.65, p-value: 0.0, FDR : 0.0

miR-10b vs. CO

HALLMARK_EPITHELIAL_MESENCHYMAL_TRANSITION — NES: 1.96, p-value: 0.0, FDR: 0.0

HALLMARK_INTERFERON_GAMMA_RESPONSE — NES: 1.68, p-value: 0.0, FDR:0.007

Enrichment plot: HALLMARK_ALLOGRAFT_REJECTION — NES: 1.55, p-value: 0.0012, FDR: 0.017

b.

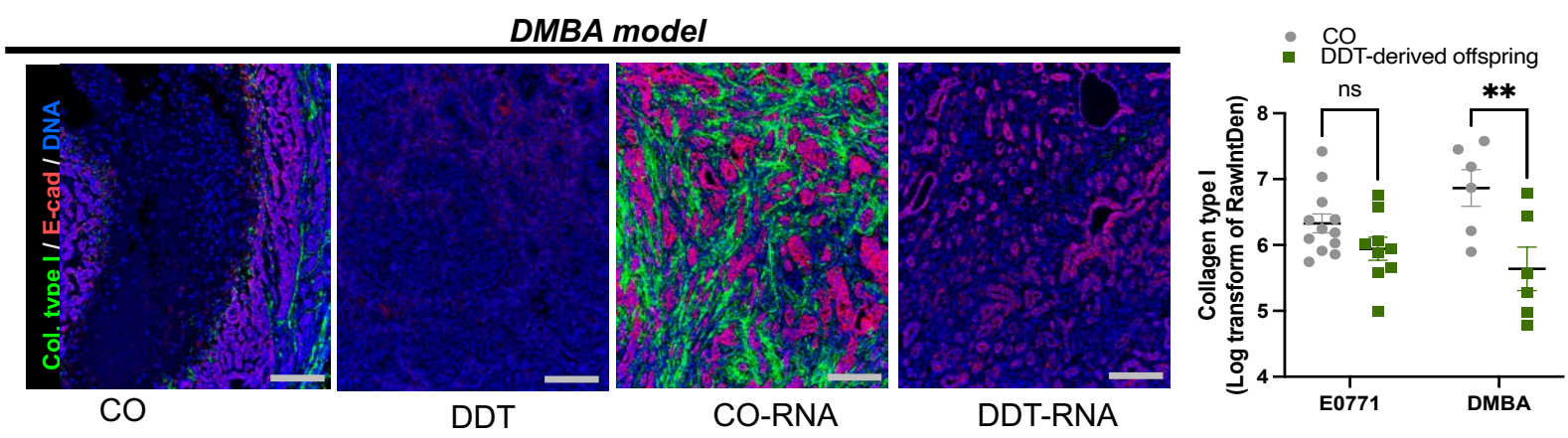

c.

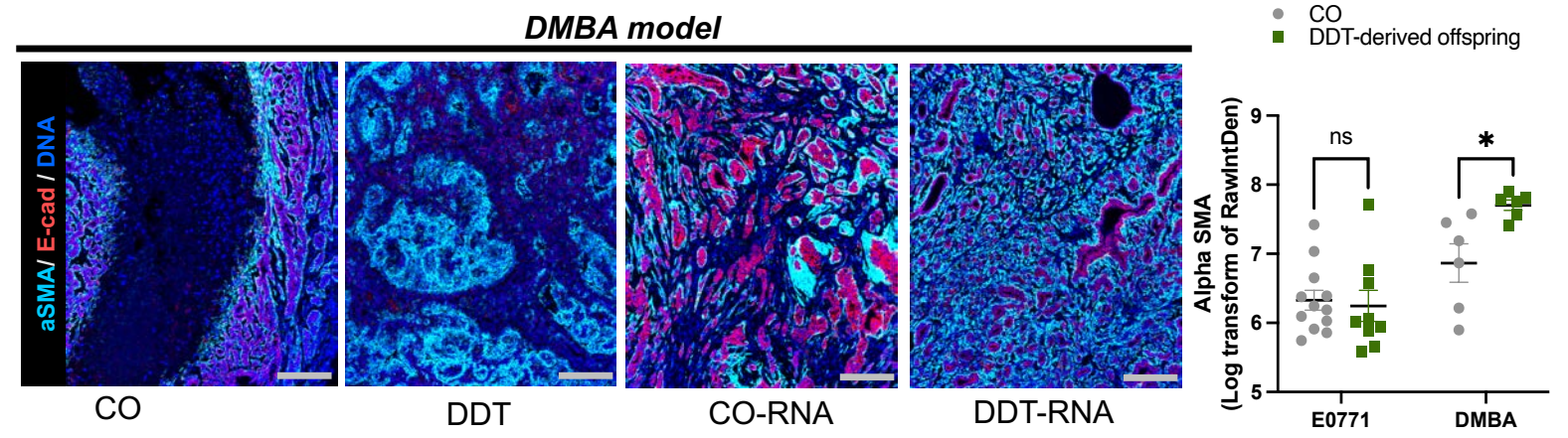

d.

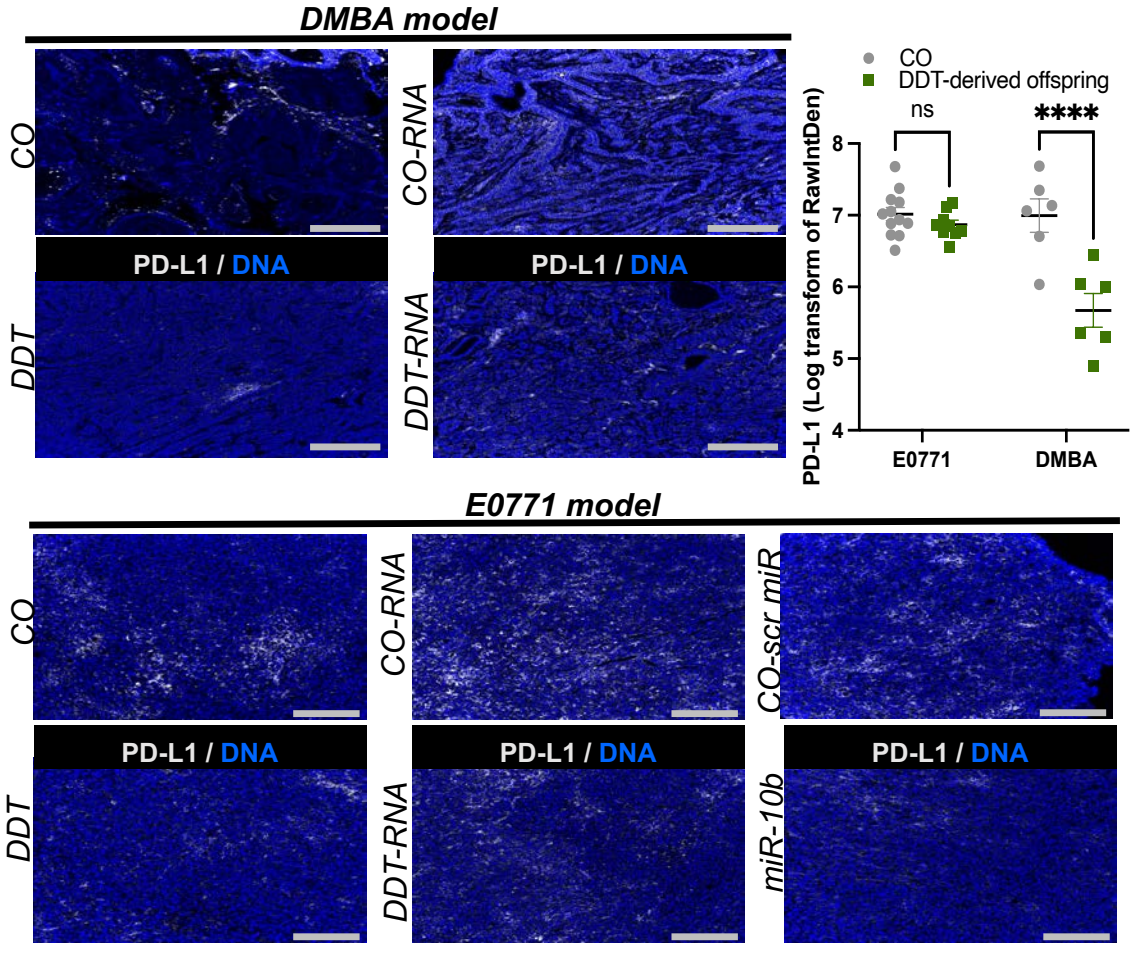

Figure 6